Proceedings of the 5th WSEAS Int. Conf. on SIGNAL, SPEECH and IMAGE PROCESSING, Corfu, Greece, August 17-19, 2005 (pp191-195)

Modeling and Measuring Uniformity of Intermetalic Formation from the Au-Al Wire Bonding Image

Omar Mohd. Rijal*, Norliza Mohd. Noor[†], Liew Kian Wah*, Omar Mohd. Badar[§]
* Institute of Mathematical Science, University of Malaya
[†]Diploma Program Studies, Universiti Teknologi Malaysia
[§]Texas Instruments (M) Sdn. Bhd.

Abstract:- The quality of wire bonding is studied by investigating the relationship between intermetallic area and compactness. A wire-bonding image was converted into its grey-scaled equivalence. Two-component mixture distributions were fitted to the two-hump brightness histogram. The fitted models are used to find the optimum threshold points which was used in defining a binary image. Percentage intermetallic was calculated from this binary image. From the same image a statistic called compactness was defined as an indicator or measure of uniformity of intermetallic formation. The results suggest both percentage intermetallic and compactness should be considered while accessing the quality of the Au-Al bond.

Key-Words:- Wire Bonding, intermetallics formation, mixture distribution, percentage intermetallic, compactness.

1 Introduction

Wire bonding is an electrical interconnection technique in joining thin wires between electrical device and its conducting track. Gold (Au) and aluminium (Al) interconnections are commonly found in the process; in which thin gold wires are welded to an aluminium pad under a combination of heat, pressure and/or ultrasonic energy.

In examining the quality of wire bond, variables such as thickness [1], and circumference [2] of intermetallics have been studied. Suresh *et al*.[3] found that the bond quality is characterized by the intermetallic coverage in two ways that is, by the percentage of the intermetallic coverage and the uniformity of the coverage. Bonds with uniform intermetallic coverage show stronger bond shear strength than bonds with spotty intermetallic region. These latter 2 variables form our main focus in this study.

Colour wire bond images provided by a semiconductor production plant will be studied. These images were taken by high-powered microscope on the gold balls that were etched from the aluminium pad. Colours of the intermetallic compounds in the images are shown in Table 1, [4].

After some noise cleaning process and transformation, a brightness histogram can be drawn from the grey-scale image, where the horizontal axis represents the brightness levels while the vertical axis represents the number of pixels in the whole image with corresponding brightness level.

Table 1 Au-Al intermetallic compounds and their corresponding colours.

Intermetallic compound	**Colour**
Au_5Al_2	Tan
Au_4Al	Tan
Au_2Al	Tan
$AuAl$	White
$AuAl_2$	Purple

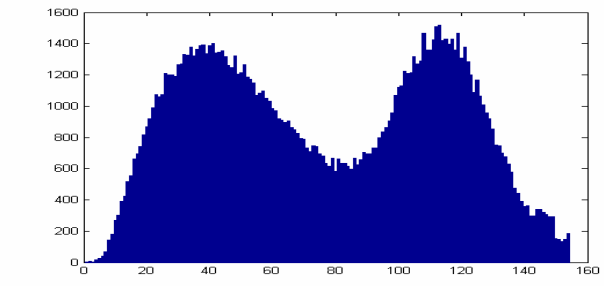

Fig. 1 Brightness histogram of a wire bond image.

2 The Normal-Normal Mixture Model

We fit a mixture distribution to the histogram with, $f(x)=\sum_{i=1}^{k} p_i g_i(x)$, where $0<p_i<1$ such that $\sum_{i=1}^{k} p_i = 1$ and $g_i(x)$ are probability density function of population π_i.

[5] has given a comprehensive description to the method in finding the maximum likelihood estimates of parameters. The maximum likelihood estimator for p_i is found to be

$$\hat{p}_i^{\,new} = \frac{1}{n}\sum_{j=1}^{n} \frac{\hat{p}_i^{\,old} g_i(x_j)}{f(x_j)} \qquad (1)$$

while the other estimates of parameter must satisfy the following equation

$$\sum_{j=1}^{n} \frac{p_q \frac{\partial}{\partial \theta_{qm}} g_q(x_j)}{f(x_j)} = \mathbf{0} \qquad (2)$$

Equation (1) and (2) will be used to find the estimates of the parameters by expectation maximization (EM) algorithm. The initial estimate of parameters can be found by using respective sample statistics by first setting a suitable threshold point.

3 THE ALGORITHM

Step1:

a) The initial estimates of parameters will be treated as old estimates and substitute into (1) to update the value of $\hat{p}_1$.

b) The updated value of $\hat{p}_1$ together with others initial estimates will be substitute in (2) to revise the value of $\hat{\mu}_1$.

c) The revised $\hat{\mu}_1$ obtained from b) will replace the initial estimates of $\hat{\mu}_1$. This revised $\hat{\mu}_1$ together with others initial estimates will be substituted in (2) again to revise the other values of parameters one at a time until all have been updated.

Step 2:

The estimation process stops if the following are satisfied (otherwise Step 1 will be repeated):

$$\begin{cases} |\hat{p}_1^{\,new} - \hat{p}_1^{\,old}| < 0.00001 \\ |\hat{\mu}_1^{\,new} - \hat{\mu}_1^{\,old}| < 0.0001 \\ |\hat{\mu}_2^{\,new} - \hat{\mu}_2^{\,old}| < 0.0001 \\ |\hat{\sigma}_1^{\,2(new)} - \hat{\sigma}_1^{\,2(old)}| < 0.001 \\ |\hat{\sigma}_2^{\,2(new)} - \hat{\sigma}_2^{\,2(old)}| < 0.001 \end{cases}$$

The fitted model is checked by performing Komogolov-Smirnov test. The number of pixels in the image is taken to be the number of samples. The large sample size leads to the rejection of the model for all images. The Komogolov-Smirnov statistics lie in the range from 0.0113 to 0.0541 whereas the critical points ranged from 0.00393 to 0.00479.

Graphs of fitted normal mixture model and empirical density function are shown in Fig. 2.

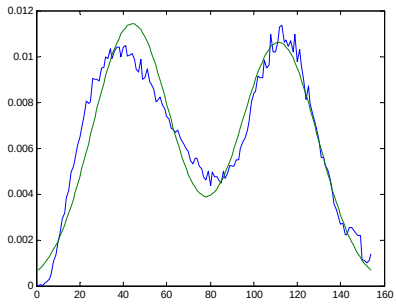

Fig. 2 The line graph of brightness levels(blue) and the fitted model (green) for s101a.jpg.

From the Komogolov-Smirnov statistics we see that the distribution of the model differs from the actual ogive only in small numbers from 0.0113 to 0.05405. This implies that our fitted mixture distribution are good approximation to the data.

4 THE GAMMA-GAMMA MIXTURE MODEL

The probability density function of a gamma distribution $\Gamma(\alpha,\lambda)$ is given by $f(x)=\frac{\lambda^{\alpha} x^{\alpha-1} e^{-\lambda x}}{\Gamma(\alpha)}$, for $x>0$. Hence, the probability density function of the mixture model of two gamma distributions is given by

$$f(x)=\frac{p_1 \lambda_1^{\,\alpha_1} x^{\alpha_1-1} e^{-\lambda_1 x}}{\Gamma(\alpha_1)} + \frac{(1-p_1)\lambda_2^{\,\alpha_2} x^{\alpha_2-1} e^{-\lambda_2 x}}{\Gamma(\alpha_2)} \qquad (3)$$

Parameter estimation was performed as before. Fig. 3 shows an example of the fitted model.

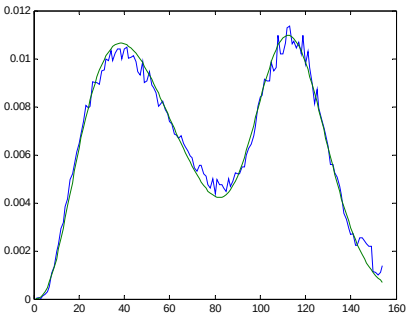

Fig. 3 The line graph of brightness levels (blue) and the fitted gamma mixture model (green) for s101a.jpg.

We observe from the Komogolov-Smirnov statistic that, the gamma models seem to fit certain groups of wire bonding images better than the normal mixture models even though it still suggests rejection of the mixture model at significant level 0.01. For other groups of images, the model shows even bigger deviation from the brightness density compare to the two-component normal mixture models.

5 THE BINARY IMAGE

Having fit a mixture distribution, the threshold point between intermetallics and background is derived [6] using the following rule

$$x \in R_1 \text{ if } \frac{f_1(x)}{f_2(x)} \geq \left(\frac{p_2}{p_1} \right), \text{ otherwise } x \in R_2 \qquad \text{- (4)}$$

where $f_j(x)$ is the probability distributions for π_j $(j = 1, 2)$. Equation 4 was applied separately to both cases of normal mixtures and gamma mixtures (i.e. equation 3).

Using a thresholds point, we can set all those pixels with brightness level less than it 0 while all pixels with brightness level higher or equal to it 1. Thus getting a binary image, denoted by BI. The ratio of zeros to the total number of pixels in the binary image BI gives the percentage intermetallic of the wire bond. Fig. 5 shows the original image and its binary counterpart.

The wire bonds that we study are products of different machines. We will label the image according to the machine that produces them, namely, by using alphabet A, B, C, D and E. We find that the gamma mixture model gives larger value of threshold points for most of the images as compare to the normal mixture model. This could be caused by the positively skewed property of the gamma probability density function.

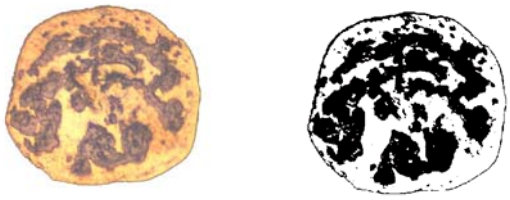

Fig. 5 Original wire bonding image and its binary counterpart.

6 EDGE DETECTION

In Fig. 6, the shaded pixels can be regarded as the neighborhood of the pixel at the center. A pixel is said to be a point on the edge when it has different pixel values with any one of the pixels in its neighborhood. From the binary image BI, we proceed by searching the pixels one by one starting from the upper left corner to the lower right.

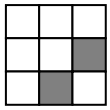

Fig 6 Defining the neighborhood of a pixel

Let BI(x, y) represent the brightness level of the (x, y) pixel which is either 1 or 0 in the binary image BI. We will create a new matrix E whose value at the (i, j) location is 0 if and only if a pixel located at (i, j) in BI satisfy

| 2*BI(i, j) - BI(i+1, j) - BI(i, j+1)) | > 0.

The condition above is actually an alternative way to say if any of the values of the pixel BI(i+1, j) or BI(i, j+1) is/are not the same as the value of pixel BI(i, j) then E(i, j) will be marked as boundary. All others pixels will be given value 1.

From the image BI and E that we obtained, we can count the area and perimeter of the intermetallic region. The number of 0 in the BI image will be regarded as the area of the intermetallic region while the number of 0 in the E image will be treated as the length of the perimeter.

7 COMPACTNESS

In pattern recognition, compactness is one of the indicators used to described the feature of an image. Compactness of a region is defined by $\frac{perimeter^2}{4\pi \times area}$. The formula can also be written in the form $\frac{\frac{perimeter^2}{4\pi}}{area}$ where the numerator is the area of circle that can be bounded by a particular perimeter. The compactness is thus represent the ratio of the area of a circle bounded by a particular perimeter and the area of the shape bounded by the same perimeter. It reflects the efficiency in using the perimeter in bounding an object. [7]

A perfect circle has compactness equal to 1, the compactness become bigger and bigger when the image has curly and twisted boundary. Therefore by find the compactness of an image we can measure the degree of 'twist' and uniformity of an intermetallic coverage.

In Figure 7, the compactness measure of two wire bond images is calculated. It is obvious that the image with densely distributed and higher percentage intermetallic produce smaller compactness whereas the one with lower percentage intermetllic and scattered intermetallic coverage gives much higher compactness measure.

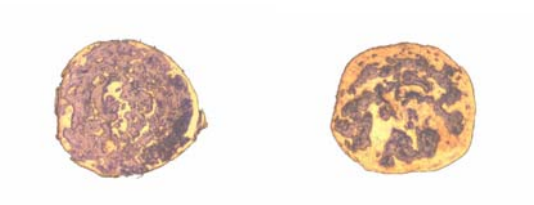

(a) (b)

Fig. 7 (a) S201a.jpg, Compactness = 50
(b) S101a.jpg, Compactness = 150.

Figure 8 gives the scatter plot of percentage intermetallic and compactness. The scatter plot above may suggest that when the percentage intermetallic is high, the compactness remains small. However, when percentage intermetallic drops below certain level, the fluctuations can be quite big. It implies that when the percentage intermetallic is low, there can be bigger chance to get a badly bonded wire.

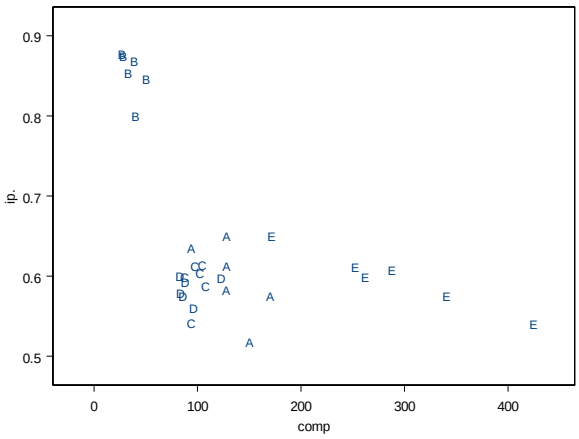

Fig. 8 Scatter plot of percentage intermetallic versus compactness for normal mixture model.

8 RESULTS AND DISCUSSION

It is well established that a high quality wire bond is characterized by high percentage intermetallic (%IM) areas and uniform coverage of intermetallics (low compactness). This study has shown that both %IM and compactness should be simultaneously considered to determine quality of wire-bond. To estimate %IM and compactness, 2-component normal mixtures and 2-component gamma mixtures were fitted. The threshold from gamma mixture tends to be slightly higher than that for the normal mixtures. Nevertheless the %IM from both model were similar in most cases. The threshold derived was used to transform the original image to a binary image from which %IM and compactness were calculated.

9 REFERENCE

[1] Ramsey, T., C. Alfaro and Dowell, H., "Metallurgy's Part in Gold Ball Bonding", *Semiconductor International*, April 1991, pp. 98-102.

[2] Clatterbaugh, G. V., Weiner, J. A. and Charles, H. K., "Gold-Aluminum Intermetallic: Ball Bond Shear Testing and Thin Film Reactions Couples", IEEE Trans. On Components, Hybrids, and Manufacturing Technology, No. 4, 1984, pp. 349-356.

[3] Suresh Kumar, Frank Wulff & Klaus Dittmer, *Degradation of Small Ball Bonds due to Intermetallic Phase(IP) Growth*, Kulicke & Soffa. http://www.kns.com/resources/articles/kumar.pdf

[4] Philofsky, E., Intermetallic Formation in Gold-Aluminum Systems, *Solid State Electronics*, Vol. 13, 1970, 1391-1300.

[5] Everitt, B.S. & Hand, D.J. (1981). *Finite Mixture Distributions*. London: Chapman and Hall Ltd.

[6] Richard A. Johnson & Dean W. Wichern (2002), *Applied Multivariate Statistical Analysis*, Fifth Edition, Pearson Education International.

[7] Mark Nixon & Alberto Aguado (2002), *Feature Extraction and Image Processing*, Newnes, United Kingdom.